EMPA20140434

AGU PUBLICATIONS

Geophysical Research Letters

RESEARCH LETTER
10.1002/2014GL060754

**Key Points:**
- Near-zero $CCl_4$ bottom-up emissions cannot be reconciled with observations
- The observed inter-hemispheric gradient can be used to quantify $CCl_4$ emissions
- The likely mean $CCl_4$ global emissions are 39 Gg/yr and lifetime is 35 years

**Supporting Information:**
- Readme
- Text S1

**Correspondence to:**
Q. Liang,
Qing.Liang-1@nasa.gov

**Citation:**
Liang, Q., P. A. Newman, J. S. Daniel, S. Reimann, B. D. Hall, G. Dutton, and L. J. M. Kuijpers (2014), Constraining the carbon tetrachloride ($CCl_4$) budget using its global trend and inter-hemispheric gradient, *Geophys. Res. Lett.*, *41*, 5307–5315, doi:10.1002/2014GL060754.

Received 6 JUN 2014
Accepted 14 JUL 2014
Accepted article online 16 JUL 2014
Published online 30 JUL 2014

# Constraining the carbon tetrachloride ($CCl_4$) budget using its global trend and inter-hemispheric gradient

**Qing Liang[1,2], Paul A. Newman[1], John S. Daniel[3], Stefan Reimann[4], Bradley D. Hall[5], Geoff Dutton[5,6], and Lambert J. M. Kuijpers[7]**

[1]Atmospheric Chemistry and Dynamics Laboratory, NASA Goddard Space Flight Center, Greenbelt, Maryland, USA, [2]Universities Space Research Association, GESTAR, Columbia, Maryland, USA, [3]Earth System Research Laboratory, Chemical Sciences Division, National Oceanic and Atmospheric Administration, Boulder, Colorado, USA, [4]Empa, Swiss Federal Laboratories for Materials Science and Technology, Dübendorf, Switzerland, [5]Earth System Research Laboratory, Global Monitoring Division, National Oceanic and Atmospheric Administration, Boulder, Colorado, USA, [6]Cooperative Institute for Research in Environmental Sciences, University of Colorado, Boulder, Colorado, USA, [7]Technical University, Eindhoven, Netherlands

**Abstract** Carbon tetrachloride ($CCl_4$) is a major anthropogenic ozone-depleting substance and greenhouse gas and has been regulated under the Montreal Protocol. However, the near-zero 2007–2012 emissions estimate based on the UNEP reported production and feedstock usage cannot be reconciled with the observed slow decline of atmospheric concentrations and the inter-hemispheric gradient (IHG) for $CCl_4$. Our 3-D model simulations suggest that the observed IHG ($1.5 \pm 0.2$ ppt for 2000–2012) is primarily caused by ongoing current emissions, while ocean and soil losses and stratosphere-troposphere exchange together contribute a small negative gradient (~0 – −0.3 ppt). Using the observed $CCl_4$ global trend and IHG, we deduce that the mean global emissions for the 2000–2012 period are $39^{45}_{34}$ Gg/yr (~30% of the peak 1980s emissions) and a corresponding total lifetime of $35^{32}_{37}$ years.

## 1. Introduction

Carbon tetrachloride ($CCl_4$) is primarily used as a feedstock or processing agent but has also been used as a cleaning agent and solvent [*CTOC Report, UNEP*, 2011]. $CCl_4$ is recognized as both an ozone-depleting substance (ODS) and greenhouse gas. As of 2008, $CCl_4$ accounted for ~11% of total tropospheric chlorine [*WMO*, 2011]. The ozone depletion potential (with respect to CFC-11) is 0.82 [*WMO,* 2011], and the 100 year global warming potential is 1400 [*WMO*, 2011]. In 1987, the Montreal Protocol (MP) included $CCl_4$, and production and consumption were eliminated for developed countries in 1996. Developing countries (i.e., Article 5 countries) were allowed a delayed reduction, but $CCl_4$ was fully banned in 2010. $CCl_4$ continues to be legally used as a contained feedstock, e.g., for hydrofluorocarbon production, since feedstock uses are not regulated.

$CCl_4$ primary sinks include stratospheric photolysis and ocean and soil degradation. The current best estimate of total lifetime ($\tau_{CCl4}$) is $25^{31}_{21}$ years [*SPARC*, 2013]. Partial lifetimes due to atmospheric photolysis ($\tau_{atmos}$), the ocean sink ($\tau_{ocean}$), and the soil sink ($\tau_{soil}$) are $44^{58}_{36}$ years [*SPARC*, 2013], $81^{167}_{71}$ years [*SPARC*, 2013], and $195^{907}_{108}$ years [*WMO*, 2011], respectively (subscripts and superscripts denote 1-$\sigma$ range).

MP controls have led atmospheric $CCl_4$ to decline at ~ 1% per year [*WMO*, 2011]. Current bottom-up emissions, estimated based on reported production and feedstock usage, were zero after 2007 [*WMO*, 2011]. There are no known substantial stocks in existing equipment or storage containers. A $\tau_{CCl4} \sim 25$ years implies a 4% per year decrease rather than the observed 1%. The 2007–2012 top-down emissions estimate derived using atmospheric observations and the current $\tau_{CCl4}$ estimate was upward of 50 Gg per yr (Gg/yr) [*WMO*, 2011]. This very large emissions estimate difference is equivalent to ~1600 railroad tank cars of liquid $CCl_4$. *Fraser et al.* [2014] suggested that contaminated soils, toxic waste treatment facilities, and possibly chloro-alkali plants emissions could contribute 10–30 Gg/yr. *De Blas et al.* [2011] also observed excess $CCl_4$ above background in Bilbao, Spain, and attributed this to an unidentified source near the measurement site. *Odabasi* [2008] found that mixing bleach with surfactants or soap could form $CCl_4$. Unintentional $CCl_4$ feedstock emissions are highly uncertain [*TEAP*, 2011] but have been estimated to be approximately 0.5% of the total feedstock used (equivalent to 5 Gg/yr for 2011 production) [*Miller and Batchelor*, 2012]. None of


©2014. American Geophysical Union. All Rights Reserved.

these potential sources alone can fully explain the 50 Gg/yr discrepancy between top-down and bottom-up emissions estimates.

In this paper, we use available source and sink data in a global 3-Dimensional (3-D) Chemistry Climate Model (CCM) to test existing emissions and lifetime estimates against $CCl_4$ mixing ratio observations. The model simulations used herein are described in section 2. Section 3 describes the use of the observed inter-hemispheric gradient (IHG) to estimate likely emissions and then the corresponding lifetime to match the observed trend. A discussion on current gaps between bottom-up and top-down emissions and lifetime estimates is in section 4 with conclusions in section 5.

## 2. Model and Simulations

Our simulations are conducted with the NASA 3-D GEOS Chemistry Climate Model (GEOSCCM) Version 2 (see supporting material A), which couples the GEOS-5 GCM [*Reinecker et al.*, 2008] with a detailed stratospheric chemistry module [*Douglass and Kawa*, 1999]. A CCM comprehensive evaluation shows that GEOSCCM agrees well with meteorological, transport-related, and chemical diagnostic observations [*Eyring et al.*, 2006]. Of particular importance, GEOSCCM represents the mean atmospheric circulation as demonstrated by its realistic age-of-air, and further, realistic loss and ODS lifetimes [*Waugh et al.*, 2007; *Douglass et al.*, 2008; *Chipperfield et al.*, 2014]. GEOSCCM also reasonably simulates inter-hemispheric transport and the observed ODS IHG [*Liang et al.*, 2008; *Chipperfield et al.*, 2014]. A GEOSCCM simulation with flux-based $CCl_3F$ (CFC-11) and $CCl_2F_2$ (CFC-12) shows that the model CFC IHGs between 1995 and 2012 compare well with the National Oceanic and Atmospheric Administration—Global Monitoring Division (NOAA GMD) observations [*Montzka et al.*, 1999; *Thompson et al.*, 2004] (see supporting material A).

Five GEOSCCM $CCl_4$ simulations were performed using geographically resolved emissions from *Xiao et al.* [2010] (Table 1). Baseline Run A is a 58 year simulation (1960–2017) with the *SPARC* [2013] photochemistry and soil lifetime, and the *WMO* [2011] ocean lifetime. Note that our modeled lifetimes differ slightly from the recommendations due to the geographic inhomogeneity in surface concentrations as well as how lifetimes are calculated, i.e., model vs. model and observation combined (supporting material A). Four 18 year (1995–2012) runs, B–E, are initialized with January 1995 Run A initial condition but with varying lifetimes, global emissions, and emission distributions, to examine their impact on the $CCl_4$ budget. The $CCl_4$ global annual emissions used in all runs, except Run E, are top-down emissions estimates derived with the global one-box model used in recent WMO Ozone Assessments [*Velders and Daniel*, 2014]—yielding $CCl_4$ declines that match the GMD observations (Figure 1a). The GMD data are from in situ measurements and flasks [*Hall et al.*, 2011]. Run E uses reduced global emissions ~ 35 Gg/yr for 1995–2012 and a lifetime of 26 years based on *SPARC* [2013]. Its $CCl_4$ decreases at ~ 2.2 ppt/yr—double the observed rate (Figure 1a). This result confirms the existing $CCl_4$ budget gap: low emissions and the current 25 year lifetime yield a global trend inconsistent with observations. We ran the last five years (2013–2017) of Run A with zero emissions, to quantify the part of the IHG due to processes other than emissions, i.e., inter-hemispheric differences in ocean and soil losses and stratosphere-troposphere exchange (STE).

## 3. Constraining the $CCl_4$ Budget Using Its Global Trend and Inter-Hemispheric Gradient

### 3.1. The Inter-Hemispheric Gradient of $CCl_4$

The IHG is recognized as a qualitative emissions indicator for long-lived compounds [*Lovelock et al.,* 1973]. Our simulations show a compact linear relationship between model annual IHG and annual global emissions for all runs ($r = 0.92$–$0.97$ for Runs A–E) (Figure 1b), despite their various emissions and lifetimes. All five runs yield very similar IHG-emissions regression slopes (0.041–0.047 ppt/Gg $yr^{-1}$) and zero-emission intercepts (−0.09 to −0.26 ppt) (Figure 1b and Table 1).

The rate of change for atmospheric mixing ratios of a long-lived compound, e.g., $CCl_4$, in the two hemispheres is expressed as:

$$\frac{\partial C_n}{\partial t} = f(EF_n)\ \ E - C_n\left(\alpha_{n,ocean} + \alpha_{n,soil}\right) - C_n\alpha_{n,STE} - (C_n - C_s)/\tau_{ns} \quad (1)$$

$$\frac{\partial C_s}{\partial t} = f(1 - EF_n)E - C_s\left(\alpha_{s,ocean} + \alpha_{s,soil}\right) - C_s\alpha_{s,STE} - (C_s - C_n)/\tau_{ns} \quad (2)$$


©2014. American Geophysical Union. All Rights Reserved.

Geophysical Research Letters

10.1002/2014GL060754

**Table 1.** A Description of the Five 3-D GEOS Chemistry Climate Model (GEOSCCM) $CCl_4$ Simulations Used in This Work

| | Description | Simulation Period | Average Emission 1995–2012 (Gg/yr) | Northern Hemisphere (NH) Emission Fraction ($EF_n$) | Lifetime $\tau$ (year) | Partial Lifetimes (year) | | | $a$ (ppt Gg/yr) | $b$[g] (ppt) | $\tau_{ns}$ (yr) |
|---|---|---|---|---|---|---|---|---|---|---|---|
| | | | | | | $\tau_{atmos}$ | $\tau_{ocean}$ | $\tau_{soil}$ | | | |
| Run A | Baseline simulation. | 1960–2017 | 64[a] | 0.937 | 25.8 | 47 | 79 | 201 | 0.047 ± 0.003 | −0.23 ± 0.19 | 1.37 |
| Run B | Decreased ocean loss. Decreased atmospheric loss forced by reduced photolysis rate. | 1995–2012 | 35[b] | 0.937 | 36.5[c] | 62[c] | 160[c] | 201 | 0.044 ± 0.005 | −0.16 ± 0.17 | 1.27 |
| Run C | Repartitioning of emissions into the Southern Hemisphere (SH) with reduced global emissions. | 1995–2012 | 50[e] | 0.882 | 30.7[d] | 47 | 160[d] | 201 | 0.041 ± 0.003 | −0.26 ± 0.17 | 1.35 |
| Run D | [f]As Run C, but with latitude-dependent ocean loss rates with faster degradation in the SH. | 1995–2012 | 50 | 0.882 | 29.5 | 47 | 135 | 201 | 0.044 ± 0.003 | −0.09 ± 0.16 | 1.44 |
| Run E | Same lifetimes as in Run A but with reduced emissions as in Run B. This simulation does not match the observed $CCl_4$ decline. | 1995–2012 | 35 | 0.937 | 25.8 | 47 | 80 | 201 | 0.044 ± 0.005 | −0.09 ± 0.18 | 1.28 |

[a]The global one-box model top-down emissions estimate for $\tau \sim 25.8$ years.
[b]Inter-hemispheric gradient (IHG)-based annual emissions calculated using the average of observed IHG from the NOAA GMD network and the Advanced Global Atmospheric Gases Experiment (AGAGE) network.
[c]$\tau$, $\tau_{atmos}$, and $\tau_{ocean}$ are determined using the global one-box model with the IHG-based emissions and the observed global trend.
[d]For Run C, $\tau_{ocean}$ is determined using the global two-box model by matching the observed IHG.
[e]The global one-box model top-down emissions estimate for $\tau \sim 30.7$ years.
[f]The latitude-dependent ocean loss rates used are $1/288\,yr^{-1}$ for 45°N –90°N, $1/222\,yr^{-1}$ for 0°N–45°N, $1/122\,yr^{-1}$ for 0°S–45°S, and $1/75\,yr^{-1}$ for 45°S–90°S. The relative strength of latitude-dependent loss rates are provided by Shari Yvon-Lewis (personal communication) and then scaled to give a 135 year $\tau_{ocean}$.
[g]The combined contribution of ocean and soil losses and stratosphere-troposphere exchange (STE) to $CCl_4$ IHG.

©2014. American Geophysical Union. All Rights Reserved.

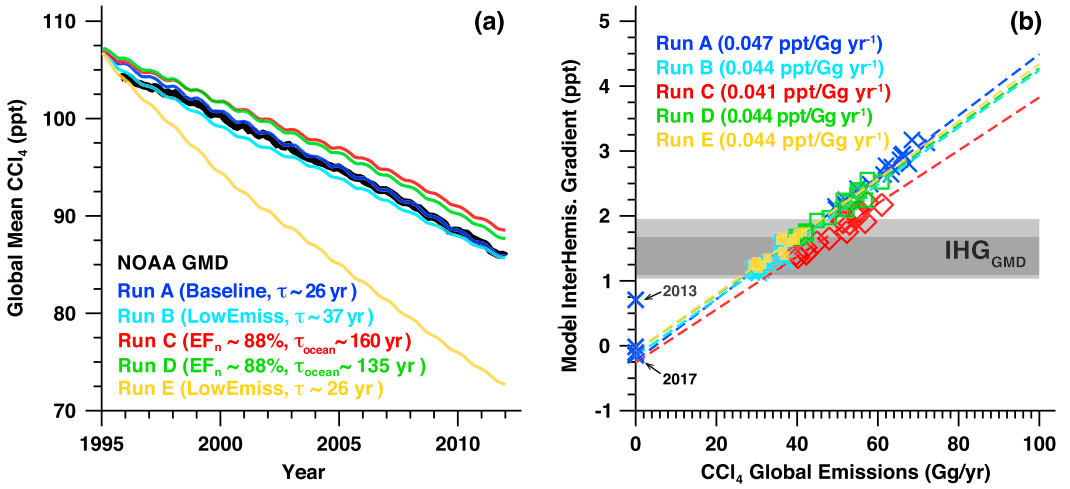


**Figure 1.** (a) The global mean $CCl_4$ mixing ratios from NOAA GMD stations (thick black line) and the 3-D GEOS Chemistry Climate Model (GEOSCCM) model runs A–E. (b) The scatter diagram of the 1995–2012 model mean inter-hemispheric gradient (IHG) vs. global emissions. Symbols represent annual-averaged values. Thick blue crosses on the *y* axis are annual mean IHGs for 2013–2017 from Run A with zero emissions. The deviation of the 2013 point from the linear regression line is due to the time needed to adjust to the abrupt change in emissions from ~50 Gg/yr to zero. IHG-emission regression lines are also shown (same color as the symbols for each run, regression slopes in parentheses). The horizontal light (dark) gray shading indicates the 2-$\sigma$ range of GMD observed IHG for 2000–2012 (2007–2012).

where $C_n$ and $C_s$ are annual mean Northern Hemisphere (NH) and Southern Hemisphere (SH) mixing ratios, respectively, inter-hemispheric exchange timescale is $\tau_{ns}$, $E$ represents global annual emissions, and $EF_n$ is the NH emissions fraction. The coefficient $f$ (=$7.9\times10^{-2}$ ppt/Gg for $CCl_4$) is a scaling factor for converting emissions to mixing ratios [*Velders and Daniel*, 2014]. Ocean ($\alpha_{ocean}$) and soil ($\alpha_{soil}$) losses have subscripts $n$ and $s$ to denote hemispheres. STE also decreases surface concentrations via dilution of tropospheric air with aged stratospheric air that is depleted of long-lived ODSs [*Nevison et al.*, 2007; *Liang et al.*, 2008]. We express the decrease in surface mixing ratios associated with STE as $-C_n\alpha_{n,STE}$ and $-C_s\alpha_{s,STE}$.

Subtracting equation (2) from equation (1) yields the IHG rate of change:

$$\frac{\partial(\Delta C_{n-s})}{\partial t} = f(2EF_n - 1)E + \Delta C_{n-s,ocean/soil} + \Delta C_{n-s,STE} - 2\Delta C_{n-s}/\tau_{ns} \quad (3)$$

where $\Delta C_{n\text{-}s}$ is the NH-SH mixing ratio difference. We use $\Delta C_{n-s,ocean/soil}$ and $\Delta C_{n-s,STE}$ to represent the IHG due to the inter-hemispheric asymmetry associated with ocean and soil losses and STE, respectively, where $\Delta C_{n-s,ocean/soil} = C_s(\alpha_{s,ocean} + \alpha_{s,soil}) - C_n(\alpha_{n,ocean} + \alpha_{n,soil})\Delta C_{n-s,STE} = C_s\alpha_{s,STE} - C_n\alpha_{n,STE}$. STE introduces a negative IHG ($\Delta C_{n\text{-}s,STE} < 0$) at the surface since the mean Brewer-Dobson circulation features stronger horizontal mixing and downwelling in the NH, thus larger NH cross-tropopause flux [e.g., *Haynes et al.*, 1991; *Holton et al.*, 1995]. For $CCl_4$, the $\partial(\Delta C_{n\text{-}s})/\partial t$ term is small (1995–2012 mean ~ −0.03 – −0.07 ppt/yr for all model runs). As a first-order approximation, equation (3) simplifies to:

$$\Delta C_{n-s} = aE + b \quad (4)$$

where $a = \tau_{ns}f(EF_n - 0.5)$ is the slope, and $b = \frac{\tau_{ns}}{2}\Delta C_{n-s,ocean/soil} + \frac{\tau_{ns}}{2}\Delta C_{n-s,STE}$ is the zero-emission intercept (Figure 1b). Hence, from equation (4) the IHG should be linearly proportional to emissions.

STE and the surface ocean and soil losses, together, contribute a small negative Northern vs. Southern IHG, −0.09 – −0.26 ppt, as indicated by the zero-emission intercepts from all five runs. The modeled IHGs for 2013–2017 from Run A with zero emissions (heavy blue pluses on Figure 1b) decrease rapidly from 2013 to 2017 and approach the $-0.23 \pm 0.16$ ppt intercept only a couple of years after emissions cease. This confirms that the zero-emission intercept reflects the IHG due to processes other than emissions. The $b$ value from Run D ($-0.09 \pm 0.16$ ppt) is 0.17 ppt higher than that from Run C ($-0.26 \pm 0.17$ ppt), suggesting that faster loss rates in the SH ocean, particularly in the SH extratropics, led to an increased IHG, but this increase is small (< +0.2 ppt).


©2014. American Geophysical Union. All Rights Reserved.

Global emissions play the predominant role, and the $CCl_4$ IHG mainly reflects ongoing emissions. The model mean IHG decreased accordingly from 2.6 ppt for Run A, to 1.7 ppt for Run C, and 2.0 ppt for Run D, and to 1.3 ppt for Run B and 1.4 ppt for Run E, consistent with their relative global emissions strength. The minor IHG differences between runs with same global emissions reflect the secondary impacts of differences in $EF_n$, $\tau_{ns}$, and sinks.

Using the model-based regression slope (0.047 ppt/Gg $yr^{-1}$) and $EF_n$ of 0.94 for Run A, we derive a $\tau_{ns}$ of 1.37 years. The other four runs yield similar $\tau_{ns}$ of 1.27–1.44 years (Table 1). GEOSCCM results from a separate flux-based simulation also show a linear relationship between IHG and global emissions for CFC-11 and CFC-12 and similar $\tau_{ns}$ (1.39–1.40 years). The GEOSCCM $\tau_{ns}$ agrees well with multi-model mean $\tau_{ns} \sim 1.39 \pm 0.18$ years estimated using $SF_6$ [*Patra et al.*, 2011]. Emission shifts between the higher and lower latitudes in the same hemisphere can have a small impact on $\tau_{ns}$. *Patra et al.* [2011] estimated that doubling $SF_6$ sources between 0°N and 30°N from ~ 1 Gg/yr to ~ 2 Gg/yr (~6 Gg/yr global emissions), led to a $< 15\%$ decrease in $\tau_{ns}$ for $SF_6$. Similarly, loss rate changes also impact $\tau_{ns}$ slightly. For example, the Run D slightly longer $\tau_{ns}$ (1.44 years) is due to its faster ocean loss rates in the SH extra-tropics (45°S –90°S) and thus a longer time needed to communicate this loss with the NH. The small variability in $\tau_{ns}$ among our five runs mainly reflects the surface loss changes and STE dilution due to atmospheric photolysis rate changes.

### 3.2. The Global Two-Box Model

We use a global two-box model from equations (3) and (5) to simulate the IHG and long-term global trend of global mean mixing ratio ($C$) for $CCl_4$:

$$\frac{\partial C}{\partial t} = f\ E - C/(\tau_{atmos} + \tau_{ocean} + \tau_{soil}) \tag{5}$$

In equation (3), we use a north-south exchange time $\tau_{ns}$ of 1.37 years—the value derived from the 3-D CCM. The IHG associated with surface losses, $\Delta C_{n\text{-}s,Ocean/Soil}$, is calculated in the two-box model as $C_n/(\tau_{atmos} + \tau_{ocean,n} + \tau_{soil,n}) - C_s/(\tau_{atmos} + \tau_{ocean,s} + \tau_{soil,s})$, where ocean and soil partial times are scaled by their respective hemispheric ocean and soil area, as in the 3-D model. The two-box model shows that, assuming uniform surface loss rates everywhere, the IHG ($\Delta C_{n\text{-}s,Ocean/Soil}$) generated purely due to the asymmetry in the NH and SH ocean and land areas is ~ 0.3 ppt for $\tau_{ocean} = 80$ years and $\tau_{soil} = 200$ years. Using a reasonably short 80 year $\tau_{ocean}$ [*SPARC*, 2013], a 1000 year upper-limit $\tau_{soil}$ [*WMO*, 2011] and an extra +0.2 ppt to account for faster ocean loss rates in the SH, in particular the SH extratropical ocean (section 3.1), we derive that the likely upper limit for $\Delta C_{n\text{-}s,Ocean/Soil}$ is ~ 0.6 ppt. Using $\Delta C_{n\text{-}s,Ocean/Soil}$ from the two-box model calculations and $b$ values from the 3-D runs, we estimate that $\Delta C_{n\text{-}s,STE}$ is ~ −0.5 ppt for $\tau_{atmos} \sim 47$ years and present-day $CCl_4$ levels. The STE contribution is smaller (smaller $|\Delta C_{n\text{-}s,STE}|$) for a longer $\tau_{atmos}$ or lower $CCl_4$ levels (see supporting material B for information on how the two-box model IHG varies with $E$, $EF_n$, and partial lifetimes).

Using the same input parameters for Run A and Run C, i.e., partial lifetimes, global emissions, and $EF_n$, and $\Delta C_{n\text{-}s,STE} \sim -0.5$ ppt, the two-box model yields very similar IHGs, regression slopes, and zero-emission intercepts as the 3-D runs (supporting material B). This suggests that the global two-box model provides quantitatively consistent information on the IHG and its dependence on sources and sinks as the 3-D CCM.

### 3.3. Estimates of $CCl_4$ Global Emissions and Lifetime

We use the observed IHG, global mean trend, and likely $CCl_4$ emissions distribution in the two-box model to estimate likely ranges for emissions and $\tau_{CCl4}$. Figure 2 shows the two-box model calculated global trend as a function of $E$ and $\tau_{CCl4}$. Observed global mean $CCl_4$ trends from the GMD and the Advanced Global Atmospheric Gases Experiment (AGAGE) [*Prinn et al.*, 2000] networks are −1.0 – −1.2 ppt/yr (2000–2012) with annual trends range between −0.9 ppt/yr and −1.5 ppt/yr. Purple contours indicate the range of $E$ and $\tau_{CCl4}$ that would match the observed mean IHG ~ 1.5 ppt (1.1–2.0 ppt, 2-$\sigma$ range), using the current best estimate $EF_n$ of 0.94 [*Xiao et al.*, 2010]. The regime where the −0.9 and −1.5 ppt/yr trend contours intersect the purple contours (dark gray shading) outlines the most likely range of $E$ and $\tau_{CCl4}$ that can reproduce the observed trend and IHG. Assuming that 94% of the global emissions reside in the NH, the mean observed IHG and global trend averaged between the GMD and AGAGE measurements imply mean global emissions of 39 Gg/yr for the 2000–2012 period (1-$\sigma$ year-to-year variance of ±4 Gg/yr) and a corresponding $\tau_{CCl4}$ of 35 years. The IHG-based mean global emissions for the 2007–2012 period are ~ 35 Gg/yr.


©2014. American Geophysical Union. All Rights Reserved.

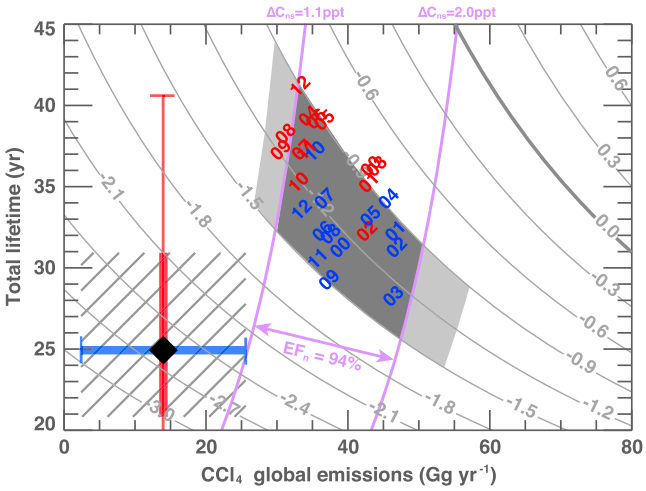


**Figure 2.** $CCl_4$ global mean trend (ppt/yr) as a function of total lifetime and emissions from the two-box model (gray contours). Purple contours indicate the emissions and $\tau_{CCl4}$ ranges that yield IHGs within the observed 1.1–2.0 ppt range (2-$\sigma$) between 2000 and 2012, using the current best estimate $EF_n$ of 0.94. Red (Advanced Global Atmospheric Gases Experiment (AGAGE)-based) and blue (GMD-based) numbers show emissions and lifetimes derived using the observed IHG and trend for individual years (2000–2012). The dark (light) gray shading outlines the range of emissions and $\tau_{CCl4}$ that can be reconciled with the observations for $EF_n$ of 0.94 (0.88–1.00). The black diamond symbol shows our current best estimate for $\tau$ (thick and thin red bars indicate 1-$\sigma$ and 2-$\sigma$ uncertainties, respectively) and the upper limit bottom-up potential emissions for 2007–2012 (thick blue bar shows 1-$\sigma$ variance) with 1-$\sigma$ uncertainty shown in black-hatched shading.

The above emissions and lifetime estimates depend upon the assumed $EF_n$, which is not accurately known. The uncertainty of our top-down $CCl_4$ global emissions and $\tau_{CCl4}$ estimates can be determined based on the likely range of $EF_n$. Using the observed IHG and the largest $EF_n$ possible—1.0, we deduce that the minimum average global emissions necessary to reproduce the atmospheric $CCl_4$ observations are ~ 34 Gg/yr ($\tau_{CCl4}$ ~ 37 years) for the 2000–2012 period. Similarly, we can derive the upper limit global emissions with a lower limit $EF_n$ estimate. ODS usages generally are thought to scale with population, and previously reported $EF_n$ for major long-lived ODSs are all ≥ 0.90 [*McCulloch et al.*, 2001, 2003; *AFEAS,* 2001]. For example, 0.96 for CFC-11 in the 1990s and 0.94 in the 2000s, 0.95 for CFC-12 in the 1990s and 0.90 in the 2000s, and 0.97 for $CH_3CCl_3$—calculated using geographically resolved emissions (courtesy of A. McCulloch and the Global Emissions InitiAtive, http://www.geiacenter.org).

The $EF_n$ lower limit (0.88) is estimated by doubling current SH emissions. This yields an upper limit global emissions estimate ~ 45 Gg/yr ($\tau$ ~ 32 years) for the 2000–2012 period. The corresponding upper and lower limits for the 2007–2012 global emissions are 31 and 40 Gg/yr, respectively.

Even when the 2007–2012 upper limit bottom-up emissions estimate (14 ± 12 Gg/yr) (section 4.1) is considered, it cannot be reconciled with observations as this magnitude of emissions yields substantially smaller IHG and a fast decline rate of ~ −2.6 ppt/yr (Figure 2).

## 4. Current Gaps

### 4.1. The Gap Between Emission Estimates

Bottom-up potential $CCl_4$ emissions were estimated to be near zero after 2007, as derived from the difference between reported production in excess of amounts used as feedstock and amounts destroyed [*WMO*, 2011]. An upper limit to potential emissions, estimated using a 2% fugitive emissions rate from feedstock and an assumed 75% destruction efficiency [*WMO*, 2011], was 34 Gg/yr for 2000–2012 (14 Gg/yr for 2007–2012). With a $\tau_{CCl4}$ ~ 25 years, the 2000–2012 top-down emissions estimate is ~ 63 Gg/yr (46–80 Gg/yr, 1-$\sigma$ uncertainty) (56 Gg/yr for 2007–2012)—a 30 Gg/yr discrepancy compared to the upper-limit bottom-up emissions. The IHG-based top-down emissions estimate from this work is $39^{45}_{34}$ Gg/yr for 2000–2012 (subscript and superscript denote the lower and upper limit estimates), which reduces the gap with bottom-up estimates. However, the 2007–2012 discrepancy remains large ($\Delta$ = ~ 20–40 Gg/yr).

The trend from bottom-up emissions estimate cannot be reconciled with the mixing ratio observations either. The observed global mixing ratios show a slow steady downward trend for 2000–2012 (Figure 3a), calculated from a least squares fit to be a 77.7 year exponential decay time scale (supporting material C), in contrast to the sharp bottom-up emissions decline from 100 Gg/yr in 1999 to 10 Gg/yr after 2008 (Figure 3c).

We de-trend the GMD surface mixing ratio observations and apply a 25 month ½-amplitude Gaussian low-pass filter to estimate year-to-year variations in anomalous abundances (deviations from the long-term trend).


©2014. American Geophysical Union. All Rights Reserved.

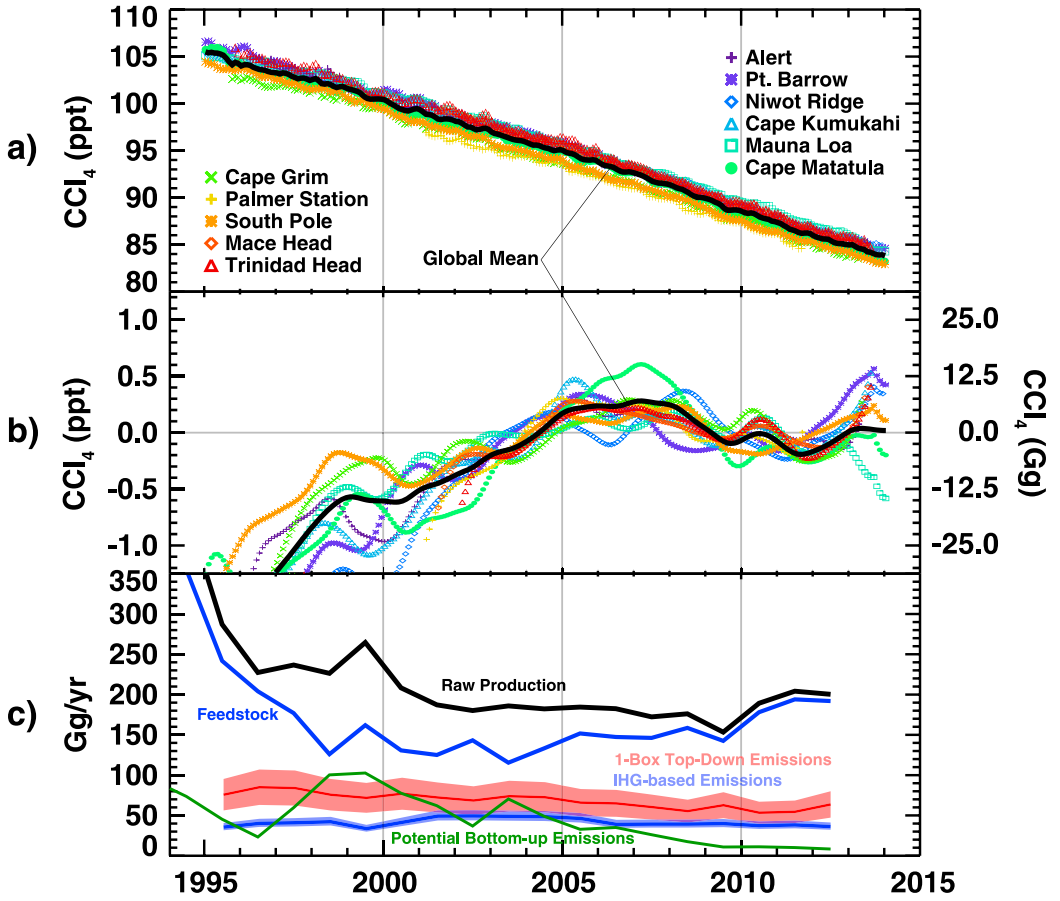


**Figure 3.** (a) Observed $CCl_4$ (NOAA GMD stations) and the global mean values (black line). (b) As Figure 3a but for mixing ratio anomalies—the right axis shows the equivalent burden anomalies (Gg). c) $CCl_4$ bottom-up and top-down emissions. Green line shows the upper limit bottom-up potential emissions estimate from reported production, feedstock usage, and the amount destroyed. The one-box model top-down emissions estimate is derived with $\tau_{CCl4}$ of $25^{31}_{21}$ years (thin red line, red shading indicates 1-sigma uncertainty due to uncertainties in lifetime and measurements). Thin blue line indicates the top-down emissions estimate (blue shading indicates lower-upper limit uncertainty estimate) derived in this work using the GMD observed IHG.

These anomalies reflect interannual variations in loss processes (surface and atmospheric) and/or emissions. The smoothing reveals three periods of change: (1) 1995–2005—steady increase in $CCl_4$ anomalies (mean ~+0.2 ppt/yr), (2) 2007–2011—small decrease (−0.1 ppt/yr), and (3) 2011–2013—an anomalous jump of +0.1 ppt/yr. Using a mixing ratio to global abundance conversion factor of $3.95 \times 10^{-2}$ ppt/Gg, these observed anomalies imply (1) ~ +5 Gg/yr increase in period 1 during 2004, (2) a ~ −3 Gg/yr decrease in 2008, and (3) an increase of +3 Gg/yr in 2012 in abundance anomalies. These observed small variations are inconsistent with the large fluctuations in bottom-up emission estimates (year-to-year changes between 10 and 30 Gg/yr for most of the years between 2000 and 2012). While inaccurate bottom-up emissions estimate is a likely cause of this inconsistency, an alternative explanation is that the year-to-year variations of loss rates may dampen large emission fluctuations. For example, a delayed atmospheric loss response (due to the required transport time from surface to the upper atmosphere, and back down to surface) can potentially offset the impact of surface emission decreases due to increased emissions in earlier years. STE interannual variability can also impact surface abundance fluctuations. This points to the need for a better understanding of the coupled impact of sources and sinks on year-to-year variations in abundances.

### 4.2. The Gap Between Lifetime Estimates

The current best estimate $\tau_{CCl4}$ of $25^{31}_{21}$ years is inconsistent with the observations, as the implied mean global emissions of $63^{46}_{80}$ Gg/yr for 2000–2012 can produce IHG matching the observations only if $EF_n$ equals $0.75^{0.85}_{0.70}$—a value much lower than those reported for major ODSs. The observed IHG and trend imply a $\tau_{CCl4}$ of 35 years (uncertainty range, 32–37 years). This requires much longer partial lifetimes than current best estimates. In Run B,


©2014. American Geophysical Union. All Rights Reserved.

we tested $\tau_{atmos}$ by increasing it from 47 years to 62 years (the upper limit for $\tau_{atmos}$). Such an increase requires a ~ 60% reduction in $CCl_4$ photolysis rate—highly unlikely as it greatly exceeds the lab-measured 15–20% cross-section uncertainty [*Rontu Carlon et al.,* 2010; *SPARC*, 2013]. High-altitude $CCl_4$ measurements are scarce, but a comparison of Run B with two balloon profiles shows a model high bias in the critical stratospheric photolysis loss region (10–70 hPa) (Figure A3). Keeping $\tau_{atmos}$ unchanged, a $\tau_{CCl4}$ of 35 years implies a need for significant increases of $\tau_{ocean}$ and/or $\tau_{soil}$ from current best estimates. This suggests a need for new measurements to re-evaluate partial lifetimes, $\tau_{ocean}$ and $\tau_{soil}$ in particular. However, it is important to note that the current 25 year lifetime estimate, even with its 2-$\sigma$ range, cannot reconcile mixing ratio observations with bottom-up emission estimates.

## 5. Summary

$CCl_4$ was increasing in the atmosphere until the early 1990s and is now in decline [*WMO*, 2011]. This decline results from regulations by the Montreal Protocol. The 1990–2006 decline was caused by an emissions decrease and loss processes [*WMO*, 2011; *SPARC*, 2013]. The current $CCl_4$ decline should be primarily determined by the lifetime, because post-2007 bottom-up emissions are estimated to be near zero. The slow ~ 1%/yr decline cannot be reconciled with our current ~ 25 year lifetime estimate (implied top-down emissions ~ 56 Gg/yr between 2007 and 2012) derived from CCMs and atmospheric, ocean, and soil observations [*SPARC,* 2013].

We simulate $CCl_4$ using a fully coupled 3-D chemistry-climate model with a state-of-the-art photochemical loss scheme, along with current estimates of ocean and soil sinks. Our CCM results show that the inter-hemispheric gradient (IHG) and the global trend provide useful information for quantitatively constraining $CCl_4$ emissions and lifetime estimates:

1. Near-zero emissions from the UNEP reported production and feedstock usage in the recent years cannot be reconciled with the observed $CCl_4$ decline, year-to-year variability, and the IHG. At a minimum, mean global emissions of 34 Gg/yr after 2000 (31 Gg/yr for the 2007–2012 period) are required to reproduce the observed IHG.
2. Ocean and soil losses contribute at most +0.6 ppt to the IHG, assuming a long soil lifetime of 1000 years (upper limit estimate) and a short ocean lifetime of 80 years (lower limit estimate) and fast loss rates in the SH ocean. Stratosphere-troposphere exchange introduces a negative gradient of about −0.5 ppt, which tends to offset the contribution from surface losses. The observed $CCl_4$ IHG mainly reflects current emissions and its NH-SH asymmetric partitioning.
3. Using the observed IHG and global trend and our knowledge of emissions distribution, we deduce that the mean global emissions during 2000–2012 are $39^{45}_{34}$ Gg/yr and a corresponding total lifetime of $35^{32}_{37}$ years. Subscript and superscript denote the lower and upper (upper and lower) limit estimates for emissions (lifetime). This would necessitate longer partial lifetimes, in particular ocean and/or soil partial lifetimes, than the current best estimates.

**Acknowledgments**
We thank Mark Schoeberl for helpful discussions and Elliot Atlas for providing balloon measurements. All data presented in this paper are available from the corresponding author upon direct request. The authors thank the referees for their valuable comments.

The Editor thanks two anonymous reviewers for their assistance in evaluating this paper.

## References

AFEAS (2001), Production, sales and atmospheric releases of fluorocarbons through 2000, Alternative Fluorocarbons Environmental Acceptability Study, Arlington, Va.

Chipperfield, M. P., et al. (2014), Multimodel estimates of atmospheric lifetimes of long-lived ozone-depleting substances: Present and future, *J. Geophys. Res. Atmos.*, *119*, 2555–2573, doi:10.1002/2013JD021097.

De Blas, M., M. Navazo, L. Alonso, N. Durana, and J. Iza (2011), Trichloroethylene, tetrachloroethylene and carbon tetrachloride in an urban atmosphere: Mixing ratios and temporal patterns, *Int. J. Environ. Anal. Chem.*, *93*(2), 228–244, doi:10.1080/03067319.2011.629346.

Douglass, A. R., and S. R. Kawa (1999), Contrast between 1992 and 1997 high-latitude spring Halogen Occultation Experiment observations of lower stratospheric HCl, *J. Geophys. Res.*, *104*(D15), 18,739–18,754, doi:10.1029/1999JD900281.

Douglass, A. R., R. Stolarski, C. Jackman, M. Gupta, P. Newman, J. Nielsen, and E. Fleming (2008), Relationship of loss, mean age of air and the distribution of CFCs to stratospheric circulation and implications for atmospheric lifetimes, *J. Geophys. Res.*, *113*, D14309, doi:10.1029/2007JD009575.

Eyring, V., et al. (2006), Assessment of temperature, trace species, and ozone in chemistry-climate model simulations of the recent past, *J. Geophys. Res.*, *111*, D22308, doi:10.1029/2006JD007327.

Fraser, P. J., et al. (2014), Australian carbon tetrachloride ($CCl_4$) emissions in a global context, *Environ. Chem.*, *11*, 77–88, doi:10.1071/EN13171.

Hall, B. D., G. S. Dutton, D. J. Mondeel, J. D. Nance, M. Rigby, J. H. Butler, F. L. Moore, D. F. Hurst, and J. W. Elkins (2011), Improving measurements of $SF_6$ for the study of atmospheric transport and emissions, *Atmos. Meas. Tech.*, *4*, 2441–2451, doi:10.5194/amt-4-2441-2011.

Haynes, P. H., M. E. McIntyre, T. G. Sheperd, C. J. Marks, and K. P. Shine (1991), On the "downward control" principle of extratropical circulations by eddy-induced mean zonal forces, *J. Atmos. Sci.*, *48*, 651–678.

Holton, J. R., P. H. Haynes, M. E. McIntyre, A. R. Douglass, R. B. Rood, and L. Pfister (1995), Stratosphere-troposphere exchange, *Rev. Geophys.*, *33*(4), 403–439, doi:10.1029/95RG02097.


©2014. American Geophysical Union. All Rights Reserved.

Liang, Q., R. S. Stolarski, A. R. Douglass, P. A. Newman, and J. E. Nielsen (2008), Evaluation of emissions and transport of CFCs using surface observations and their seasonal cycles and simulation of the GEOS CCM with emissions-based forcing, *J. Geophys. Res.*, *113*, D14302, doi:10.1029/2007JD009617.

Lovelock, J. E., R. J. Maggs, and R. J. Wade (1973), Halogenated hydrocarbons in and over the Atlantic, *Nature*, *241*, 194–196, doi:10.1038/241194a0.

McCulloch, A., P. Ashford, and P. M. Midgley (2001), Historic emissions of fluorotrichloromethane (CFC-11) based on a market survey, *Atmos. Environ.*, *35*(26), 4387–4397.

McCulloch, A., P. M. Midgley, and P. Ashford (2003), Releases of refrigerant gases (CFC-12, HCFC-22, and HFC-134a) to the atmosphere, *Atmos. Environ.*, *37*(7), 889–902.

Miller, M., and T. Batchelor (2012), Information paper on feedstock uses of ozone-depleting substances, Touchdown Consulting, Brussels, Belgium. [Available at http://ec.europa.eu/clima/policies/ozone/research/docs/feedstock_en.pdf.]

Montzka, S. A., J. H. Butler, J. W. Elkins, T. M. Thompson, A. D. Clarke, and L. T. Lock (1999), Present and future trends in the atmospheric burden of ozone-depleting halogens, *Nature*, *398*(6729), 690–694, doi:10.1038/19499.

Nevison, C. D., N. M. Mahowald, R. F. Weiss, and R. G. Prinn (2007), Interannual and seasonal variability in atmospheric N2O, *Global Biogeochem. Cycles*, *21*, GB3017, doi:10.1029/2006GB002755.

Odabasi, M. (2008), Halogenated volatile organic compounds from the use of chlorine-bleach-containing household products, *Environ. Sci. Technol.*, *42*, 1445–1451, doi:10.1021/es702355u.

Patra, P. K., et al. (2011), TransCom model simulations of $CH_4$ and related species: Linking transport, surface flux and chemical loss with $CH_4$ variability in the troposphere and lower stratosphere, *Atmos. Chem. Phys.*, *11*, 12,813–12,837, doi:10.5194/acp-11-12813-2011.

Prinn, R. G., et al. (2000), A history of chemically and radiatively important gases in air deduced from ALE/GAGE/AGAGE, *J. Geophys. Res.*, *105*(14), 17,751–17,792, doi:10.1029/2000JD900141.

Reinecker, M. M., et al. (2008), The GEOS-5 data assimilation system-documentation of versions 5.0.1, 5.1.0, and 5.2.0, *Tech. Rep. 104606*, vol. 27, NASA, Greenbelt, Md.

Rontu Carlon, N., D. K. Papanastasiou, E. L. Fleming, C. H. Jackman, P. A. Newman, and J. B. Burkholder (2010), UV absorption cross sections of nitrous oxide ($N_2O$) and carbon tetrachloride ($CCl_4$) between 210 and 350 K and the atmospheric implications, *Atmos. Chem. Phys.*, *10*, 6137–6149, doi:10.5194/acp-10-6137-2010.

SPARC (2013), The lifetimes of stratospheric ozone-depleting substances, their replacements, and related species, *SPARC Rep. 6, WCRP-15/2013*, edited by M. Ko et al., SPARC Office, Zurich, Switzerland.

TEAP (2011), *Progress Rep.*, vol. 1, coordinated by L. Kuijpers and M. Seki, Technology and Economic Assessment Panel, United Nations Environmental Programme, Nairobi, Kenya.

Thompson, T. M., et al. (2004), Halocarbons and other atmospheric trace species, in *Summary Rep. 27 2002-2003*, edited by R. C. Schnell et al., pp. 115–135, Clim. Monit. Diagn. Lab., U.S. Dep. of Commer., Boulder, Colo.

UNEP (2011), *2010 Assessment Rep.*, United Nations Environment Programme, Ozone Secretariat, Nairobi, Kenya. [Available at http://ozone.unep.org/Assessment_Panels/TEAP/Reports/CTOC/.]

Velders, G. J. M., and J. S. Daniel (2014), Uncertainty analysis of projections of ozone-depleting substances: Mixing ratios, EESC, ODPs, and GWPs, *Atmos. Chem. Phys.*, *14*, 2757–2776, doi:10.5194/acp-14-2757-2014.

Waugh, D. W., S. E. Strahan, and P. A. Newman (2007), Sensitivity of stratospheric inorganic chlorine to differences in transport, *Atmos. Chem. Phys.*, *7*, 4935–4941, doi:10.5194/acp-7-4935-2007.

WMO (2011), Scientific assessment of ozone depletion: 2010, Global Ozone Research and Monitoring Project, *Rep. 52*, World Meteorological Organization, Geneva, Switzerland.

Xiao, X., et al. (2010), Atmospheric three-dimensional inverse modeling of regional industrial emissions and global oceanic uptake of carbon tetrachloride, *Atmos. Chem. Phys.*, *10*(21), 10,421–10,434, doi:10.5194/acp-10-10421-2010.


©2014. American Geophysical Union. All Rights Reserved.